J. Fluid Mech. (1971), *vol.* 50, *part* 4, *pp.* 625–644
Printed in Great Britain

The stability of unsteady axisymmetric incompressible pipe flow close to a piston. Part 1. Numerical analysis

By J. H. GERRARD

Department of the Mechanics of Fluids,
University of Manchester

(Received 24 May 1971)

A numerical solution of the Navier–Stokes equations of motion by means of finite-difference forms of the vorticity and continuity equations is presented. This is applied to the study of the flow of an incompressible fluid produced by the motion from rest of a piston in a cylindrical tube of circular cross-section.

Experiments at high Reynolds number indicated the presence in the starting flow of a ring vortex which was not reproduced by computation. Iteration to determine the stream function was not found to be necessary to achieve 1 % accuracy. Omitting iteration is equivalent to only slightly disturbing the flow. An additional random disturbance applied to the flow at each time step was found to result in the production of the ring vortex.

1. Introduction

The problem to which the computations described in Part 1 is applied was chosen in order to develop the computational and experimental techniques. The basis of the choice of problem was that of simplicity. As it has transpired an unexpected feature of the flow at high Reynolds number has added interest as well as complexity. The physical problem will be described in detail in Part 2, which presents the experimental evidence. The investigations centre around the basic configuration of a piston advancing unsteadily in a tube of circular cross-section and concern the flow in an incompressible viscous fluid in front of the piston. Far from the piston solutions can be obtained analytically after the manner of Symanski (1930), Sexl (1930) and, more recently, Womersley (1955) and Uchida (1956) who obtained explicit solutions for sinusoidal motion. We have been concerned with flow started from rest by both impulsive and gradual motion of the piston.

The computational methods are well established. The Navier–Stokes equations are generally solved in one of two ways: either by means of the vorticity equation and the continuity equation with vorticity and stream function as the variables or more directly in terms of velocity and pressure. The latter method is more recent: see, for example, Chorin (1967). The former method, which stems from the work of Thom (1928), has been investigated much more extensively. Though originating 40 years ago interest has recently considerably increased with the

widespread use of digital computers. Different facets of treatments similar to the present one are described by Fromm & Harlow (1964), Pearson (1965), Macagno & Hung (1967), Strawbridge & Hooper (1968) and Williams (1969).

The vorticity equation and continuity equation may be solved by explicit or implicit methods. Implicit methods have the advantage of being more economical in computing time at least in principle. Pearson (1965) advocates the implicit method whereas Strawbridge & Hooper (1968) favour the explicit. We have followed the explicit method, as also did Macagno & Hung (1967), for the reasons given by Strawbridge & Hooper concerning boundary values of the vorticity. The explicit method is more straightforward and further reasons for its adoption for calculations of unsteady flow are given below in connexion with the determination of the time step. The maximum time step is usually determined from considerations of computational stability. A slightly more stringent condition arises from the requirement of faithful reproduction of the Reynolds number. In view of this the more certain approach of the explicit method is favoured. It may be that implicit methods are not subject to computational damping at large time steps but it seems that this has yet to be proved.

A simple test of the correctness of the method by the reproduction of a known analytical solution is a necessary but not strictly a sufficient proof that the program is acceptable. Peculiarities of boundary condition and stability vary from one flow to another.

The programs have been written in Atlas Autocode and run on the Manchester University Atlas computer. Run times of several minutes were required.

2. Basic equations

In an axially symmetric flow there are two velocity components, an axial velocity w and a radial velocity u. We define axes z and r in the axial and radial directions. The Navier–Stokes equations relate w and u to r and z, and include the time t, pressure p and kinematic viscosity coefficient ν. By eliminating p from the equations of motion in the two principal directions one obtains the vorticity equation:

$$\frac{\partial \eta}{\partial t}+\frac{\partial}{\partial r}(u\eta)+\frac{\partial}{\partial z}(w\eta)=\frac{1}{Re}\left(\nabla^2\eta-\frac{\eta}{r^2}\right), \tag{1}$$

where with axial symmetry

$$\nabla^2=\frac{\partial^2}{\partial r^2}+\frac{1}{r}\frac{\partial}{\partial r}+\frac{\partial^2}{\partial z^2}.$$

η is the only non-zero component of the vorticity and is $\partial u/\partial z-\partial w/\partial r$. Introducing the Stokes stream function ψ, where

$$u=\frac{1}{r}\frac{\partial \psi}{\partial z} \quad \text{and} \quad w=-\frac{1}{r}\frac{\partial \psi}{\partial r}, \tag{2}$$

the continuity equation may be written

$$\eta=\frac{1}{r}\left(\frac{\partial^2\psi}{\partial r^2}-\frac{1}{r}\frac{\partial \psi}{\partial r}+\frac{\partial^2\psi}{\partial z^2}\right). \tag{3}$$

Equations (1) and (3) are non-dimensionalized with some convenient mean velocity W and the tube diameter D, the Reynolds number is defined as WD/ν. By substituting (2) into (1) the equation is written in central finite-difference form as

$$\eta_{i,j}^{k+1}\left(1+\frac{\Delta t}{Re\,r^2}+\frac{2\Delta t(h^2+g^2)}{Re\,h^2g^2}\right)\Big/2\Delta t$$

$$=\eta_{i,j}^{k-1}\left(1-\frac{\Delta t}{Re\,r^2}-\frac{2\Delta t(h^2+g^2)}{Re\,h^2g^2}\right)\Big/2\Delta t+\{(Re\,r/4gh)\,[(\psi_{i+1,j}-\psi_{i-1,j})\,(\eta_{i,j-1}-\eta_{i,j+1})$$

$$+(\psi_{i,j+1}-\psi_{i,j-1})\,(\eta_{i+1,j}-\eta_{i-1,j})]+Re\,\eta_{i,j}(\psi_{i+1,j}-\psi_{i-1,j})/2g$$

$$+r^2(\eta_{i,j+1}+\eta_{i,j-1})/h^2+r(\eta_{i,j+1}-\eta_{i,j-1})/2h+r^2(\eta_{i+1,j}+\eta_{i-1,j})/g^2\}/(Re\,r^2). \quad (4)$$

The continuity equation becomes

$$\psi_{i,j}=\{h^2\psi_{i-1,j}+h^2\psi_{i+1,j}+g^2\psi_{i,j+1}+g^2\psi_{i,j-1}$$

$$-hg^2(\psi_{i,j+1}-\psi_{i,j-1})/2r-h^2g^2r\eta_{i,j}\}/\{2(h^2+g^2)\}. \quad (5)$$

Because of axial symmetry the equations have only to be solved in a radial plane containing the axis of the tube. The field of flow is bounded by the tube axis and wall and by two parallel radial lines, one of which lies in the piston surface. This rectangular area is divided by a rectangular mesh. The lengths h and g are the mesh lengths in the r and z directions respectively. The subscripts i, j refer to mesh points in the z and r directions respectively and the superscript refers to the number of the time step. The equation thus gives $\eta_{i,j}$ at time $(k+1)\Delta t$, where Δt is the time step, in terms of $\eta_{i,j}$ at time $(k-1)\Delta t$ and ψ and η values at adjacent points at time $k\Delta t$. The superscript k is omitted. A direct finite-difference translation of equation (1) results in more terms involving $\eta_{i,j}$ on the right-hand side of the equation. These have been transposed by means of the linear relationship

$$\eta_{i,j}^{k}=\tfrac{1}{2}(\eta_{i,j}^{k+1}+\eta_{i,j}^{k-1}).$$

This substitution increases the stability of the program. Equation (4) is similar to, but not identical with, that used by Macagno & Hung (1967) who also investigated flow in tubes of circular cross-section.

3. Method of solution

The problem is set up by assigning values of η and ψ at all points of the mesh. Equation (4) determines the value of η at one time step later. The values of η on the right-hand side of equation (4) are values at one time step earlier than the $\eta_{i,j}^{k+1}$ on the left-hand side: thus the values to be inserted in (4) are determined by the direction in which the mesh is scanned. Equation (5) determines the values of ψ corresponding to the new vorticity field (at time $(k+1)\Delta t$). As it stands (5) is only strictly true for vanishingly small time-step values because at the first calculation at the first point in the mesh the right-hand side values of ψ are ψ^k: the values calculated tend towards ψ^{k+1} if the mesh is scanned repeatedly. The program was designed to iterate the scanning of the mesh to determine ψ until

the largest change in ψ at any point was less than some prescribed value. However iteration is expensive in computing time and it transpired that iteration was not necessary because the time step had to be very small for other reasons which will be discussed below.

After the determination of the η and ψ fields in the interior of the mesh new boundary values are assigned before repeating the process to determine the progression in time.

4. The mesh size and time step

The finite-difference form of the equations must satisfy certain requirements in order to faithfully reproduce a true solution of the continuous equations. Obviously each finite-difference statement must approach the continuous statement as the mesh size and time step tend to zero. The essential requisite is that the truncation errors shall not be large, that is, that the contribution of higher order differential coefficients shall be small compared with the one which is under consideration, i.e.

$$\frac{h^3}{\Delta Z}\frac{\partial^3 Z}{\partial x^3} \ll 1, \quad \frac{\Delta t^3}{\Delta Z}\frac{\partial^3 Z}{\partial t^3} \ll 1, \tag{6}$$

since central differences remove the derivatives of even order. Z is either η or ψ and ΔZ is the change in Z in the interval of x or t. These inequalities imply that initial disturbances are always likely to have a large effect in flows started from rest where $\eta = 0$ initially and large gradients occur near boundaries. In the problem under consideration there is a region where higher derivatives are always large. This is at the intersection of the piston and the wall which are in relative motion. This singular region must be considered separately.

There is another relation connecting h and Δt which results from the condition that Reynolds number must be faithfully represented and which also relates to the truncation error. Temporal or spatial small-scale variations are smoothed out if the mesh is not fine enough. This introduces an artificial viscosity and reduces the effective Reynolds number. Any finite mesh size will reduce the effective Reynolds number *of certain flows*. This is presumably especially so at high Reynolds number at which small-scale disturbances may grow in the real flow. Certainty about the absence of this growth would seem to come only by successive reductions of the mesh length.

We turn now to the other relation which the mesh sizes h and Δt must satisfy in order that the correct Reynolds number be simulated. In an explicit method in which the change in vorticity distribution in one time step is determined by a single scan of the mesh there may be regions where the maximum rate of diffusion is limited to an advance of one mesh length per time step. This distance must be greater than the actual rate of diffusion. Thus

$$h > C(\nu t)^{\frac{1}{2}},$$

where C is approximately constant but exactly constant only for diffusion from a flat plate. The magnitude of C is of the order of 5. This results in the non-dimensionalized expression

$$\Delta t < \tfrac{1}{25} h^2 Re. \tag{7a}$$

The amount by which Δt needs to be less than this quantity for the Reynolds number to be uniformly accurate must be found by trial and depends on the particular problem. A similar limit is obtained from program stability considerations and is usually less stringent, for example, Williams (1969) obtains $\Delta t < \frac{1}{8}h^2Re$. Thoman & Szewczyk (1964), on the other hand, obtain a more stringent condition from stability considerations.

There is a restriction on the mesh size independently of Δt which arises from the truncation error and also concerns the faithful representation of the Reynolds number. In order that the truncation error of the inertia terms shall not mask the viscous terms

$$h^3Re \ll 1. \tag{7b}$$

In all the computation this condition was satisfied.

One wonders to what extent implicit methods which increase computational stability and allow longer time steps to be used are liable to this scale effect; see, for example, Pearson (1965). It would appear, however, that this effect only applies to a method which determines the progression in time by one scan of the mesh when the scan advances up the vorticity gradient.

Both implicit and explicit methods require iteration at each time step. Pearson does not quote the number of iterations required. An investigation of accuracy by varying the time step, mesh size and number of iterations reveals that in the present approach the number of iterations required is not large. The number varies during the execution of the program, but for most of the computing time one scan of the mesh determines the stream function sufficiently accurately. This was found to be the case by Chorin (1967) in direct solution in terms of velocity and pressure. This conclusion depends upon the time step and mesh length used and the information required: we have not investigated the detail of the boundary-layer flow.

5. Boundary conditions

In this section the suffix 0 will be used to denote values on the boundary. Suffixes 1 and 2 refer to values at 1 and 2 mesh lengths, h, from the boundary respectively. Equations (4) and (5) are used to determine η and ψ within the flow but not on the boundaries. The ψ values on the wall are fixed by straightforward continuity considerations. Values of η_0 are required to determine η at points adjacent to the wall at a later time. Boundary values of η are determined by extrapolation from the values in the flow.

By expanding the stream function and the vorticity at the wall in Taylor series and applying the conditions of no slip and zero normal velocity at the wall, expressions for η_0 are found in terms of adjacent values of η and ψ. In a cylindrical tube of circular cross-section these expressions are obtained as described by Macagno & Hung (1967). This method is basically that employed by Thom (1928). On the side walls of the tube the expression for vorticity is

$$\eta_0(\tfrac{1}{3}h^2r_0 - \tfrac{5}{24}h^3) = \psi_1 - \psi_0 - (\tfrac{1}{6}h^2r_0 - \tfrac{1}{3}h^3)\,\eta_1 - \tfrac{1}{24}h^4r_0\left\{\left(\frac{\partial^2\eta}{\partial r^2}\right)_0 + \left(\frac{\partial^2\eta}{\partial z^2}\right)_0\right\} + O(h^5). \tag{8}$$

This equation is the same as that of Macagno & Hung if we insert $\eta_2 = 2\eta_1 - \eta_0$ in their relation. Equation (8) is used in the form

$$\eta_0 = \frac{24(\psi_1 - \psi_0)}{h^2(4-5h)} - \eta_1 \frac{2-3h}{4-5h}, \tag{9}$$

neglecting the term of order h^4. Macagno & Hung suggest that the next term may be included by an iteration process to deal with $(\partial^2\eta/\partial z^2)_0$ but this iteration was found here to converge extremely slowly to an incorrect limit.

On the piston surface the corresponding equations for the boundary value of the vorticity, η_0, contains the gradient in the direction of the surface. The first derivative was fortunately absent from equation (8), relating to the side walls of the tube. The corresponding expression on the piston is

$$\eta_0\left(\frac{g^2 r}{3} - \frac{g^4}{24r}\right) = \psi_1 - \psi_0 - \frac{rg^2}{6}\eta_1 + \frac{g^4}{24}\left(\frac{\partial\eta}{\partial r}\right)_0 + \frac{g^4 r}{24}\left\{\left(\frac{\partial^2\eta}{\partial r^2}\right)_0 + \left(\frac{\partial^2\eta}{\partial z^2}\right)_0\right\} + O(rg^5). \tag{10}$$

By neglecting the terms of order g^4 we obtain

$$\eta_0 = 3(\psi_1 - \psi_0)/rg^2 - \tfrac{1}{2}\eta_1. \tag{11}$$

No attempt has been made to account for the radial derivatives. Equation (11) was used for those applications in which a solid piston was employed. In those cases where the 'piston' was an air–water interface the boundary condition used was that $\eta_0 = 0$ for all time. When employing (11) a computational instability arose on the piston boundary; this was so-called time-splitting and was removed in a manner adopted by some previous workers (e.g. Williams 1969). The boundary value used was the mean of the calculated value and the value obtained by extrapolation from previous times.

6. Program details

6.1. *Field of flow and mesh lengths*

In the present applications the flow is bounded by the cylinder walls and a piston. At the end of the flow remote from the piston gradients in the axial direction disappear. The boundary is defined as being where the axial gradient of the vorticity at one mesh length from the wall falls below a prescribed limit. The vorticity one mesh length further from the piston is equated to the value at the penultimate mesh point. In some calculations a fixed length in the axial direction was used.

Since gradients are expected to be changing most rapidly near the solid boundaries a variable mesh length was introduced. Mesh length in some programs was made to increase in steps which were smallest at the piston and the side wall and increased towards the axis and away from the piston. This involved special treatment of the finite-difference forms of the gradients at the intersections where mesh length changed but otherwise was straightforward.

6.2. *Initial conditions*

Except in the preliminary computations which will be dealt with separately, only flows starting from rest have been considered. In all cases the piston moves towards the fluid. At the instant of starting a flow, whether impulsively or otherwise, the vorticity at the wall is very high and a very thin boundary layer exists. This cannot be treated accurately by any finite-difference scheme. It has been modelled here by assuming a particular boundary-layer thickness and velocity distribution initially. The velocity on the side walls was assumed to increase linearly with decreasing radius from zero at the wall to that value, w_0, at one mesh from the wall which made the mean velocity equal to the piston speed. The wall vorticity was put equal to w_0/h and the value at distance h from the wall equated to one half the wall value. The vorticity on the piston surface was made equal to zero initially.

In flow near the non-uniformly moving piston a similar procedure was followed. An additional wall vorticity equal to w_0/h was added at each time step where w_0 is now the *change* in velocity in the time interval. The stream function was similarly adjusted by an increment at all points corresponding to a velocity change equal to the change in piston speed. An adjustment was made at one mesh length from the wall to account for the boundary-layer change during the previous time step.

6.3. *Treatment of the corner*

In the immediate vicinity of the corner the flow is dominated by viscosity. Batchelor (1967) considers the creeping flow in a moving corner. In the present problem the region of applicability of such an analysis is extremely small. In an idealized representation of the motion of a piston in a tube there is a singular point at the piston–wall junction where the velocity has the two values of zero and the piston speed. In a real situation there must be a gap between the piston and the wall. Relative to the advancing piston there is flow into the gap near to the wall and out of the gap near to the piston. In an attempt to explain peculiarities of the flow which were not reproduced in the numerical solution, various models of the gap flow were investigated. It was concluded that refinements in modelling the flow in the corner did not significantly improve the solution away from the immediate vicinity of the corner.

In the corner the boundary value of the vorticity rapidly changes from being large on the side wall to being large and of opposite sign on the piston. Since the vorticity must go through zero very close to the corner its value at the corner was equated to zero and constrained to remain so. The corner value could not be obtained by extrapolation from the flow in the manner of the other boundary values. In any case the extrapolation becomes inaccurate near the corner because of large gradients along the wall.

In the studies in which a free surface replaced the piston the surface vorticity was taken to be zero. In this case also, equating the corner value to zero is reasonable.

6.4. *Accuracy*

Provided that the finite-difference equations tend to the continuous equations as the mesh length and time step tend to zero, small enough increments will assure sufficient accuracy. A balance must obviously be struck between accuracy and computing time. Initial investigations were performed on a simplified program in which only radial gradients existed. This was applied to the solution of the flow far from the piston for which an analytical result exists for sinusoidal piston motion (see, for example, Uchida 1956). This work is reported briefly elsewhere (Gerrard 1971). A considerable reduction in computing time is obtained in this way, the mesh being replaced by a radial line of points.

The variable quantities affecting the accuracy and stability are the mesh length, the time step and the number of iterations used to determine the stream function. Calculations were made at two values of the number which replaces the Reynolds number in this oscillating flow. The non-dimensional group here is $D^2/\nu T$, where D is the tube diameter, ν the kinematic viscosity and T the period of oscillation. As long as there is no transition to turbulence the Reynolds number is not significant in this problem. The equation of motion is as equation (1) but with $D^2/\nu T$ replacing the Reynolds number. We put $R = D^2/\nu T$.

Computations were commenced with $h = 0{\cdot}02$. In view of the inequality (7*a*), Δt has a maximum value determined by the accuracy required. (Stability considerations are less stringent.) Initially, without any iteration to determine ψ, the error in velocity, for $h^2R/\Delta t = 146$, was $\frac{1}{2}\%$ of the maximum piston speed near the centre of the flow and $\frac{3}{4}\%$ near to the wall. Increasing $h^2R/\Delta t$ by a factor of 2, keeping h constant, slightly decreased the error near the centre of the flow to $\frac{1}{3}\%$ and had no effect near to the wall. This implies that $h^2R/\Delta t$ is large enough. Decreasing h by a factor of 2 *increased* the error by about a factor of 2 because of the fourfold decrease in $h^2R/\Delta t$. Repeating the calculation of ψ once (one iteration) produced about the same improvement as decreasing Δt, for about the same change in computing cost. Variation with each of the three parameters was slow at these values; with a much larger mesh or time step, variation became more rapid. We conclude that with reasonable lengths of computing run the accuracy must be limited to a little better than 1 %.

7. Piston started from rest: application of the basic program

Two series of experiments have been performed: a series in which the flow near a free surface was investigated and one concerning flow close to a solid piston. The experiments revealed a ring vortex when the impulsively started flow had a Reynolds number above about 450. The measurements with a solid piston were performed at a Reynolds number of 525. Numerical work was initially restricted to Reynolds numbers of 525 and 1000.

Programs were arranged to print out values of velocity components, of stream function and of vorticity, at each mesh point when desired. Some programs had the added facility of tracing particle paths for direct comparison with dye-streak photographs. In these calculations the initially chosen particles

were moved at the end of each time step with the local flow velocity for a time of one time step.

When particle drift measured at several points along an axial line at 0·8 of the radius from the centre was compared with the computed values a discrepancy was evident. This was attributed to the inability of the program to produce the ring vortex in sufficient strength. A protracted series of numerical investigations followed.

The results obtained at this stage with what may be called the basic program will be presented first. The mesh lengths were different in the axial and radial directions being equal to 0·02 and 0·0278 diameters respectively. The values of $h^2Re/\Delta t$ of 130 and 270 corresponding to these lengths were expected to be adequate and (7*b*) was satisfied; the preliminary result for an infinite tube suggested that an error of less than 1 % in the velocity may be expected. The problem here, however, is somewhat different. We are now dealing with a stability problem in which the mesh should be small compared with a much smaller scale than the diameter. It is widely recognized that digital computers are strained to their limit to accurately reproduce flows at high Reynolds number.

The results obtained with the basic program at a Reynolds number of 1000 are presented as instantaneous streamlines in figures 1 and 2 for the two cases of solid piston and free-surface boundaries. With the solid piston a circulating region develops near the piston immediately after the impulsive start and drifts away axially to die out after half a diameter of piston motion. When the piston is a free surface which allows slip this circulating region is absent, but now a circulating region appears near the side wall. The intersections of the mesh with the boundaries are shown on the figures, from which it is seen that the closed streamlines in both figures 1 and 2 are only two mesh lengths in extent in one direction. It is worth noting that at the times shown the wall boundary layer has grown to about 0·1 diameter. The impression gained by experimental observation is that the apparent vortex ring which develops after half a diameter of motion is largely independent of the piston boundary condition. For this reason a numerical experiment was performed in which marked elements were traced to see if any rolling up was evident. Figure 3 shows the first attempts. Marked fluid in a rectangle close to the wall and extending 0·4 diameter from the piston was followed. Particles close to the wall shot across the face of the piston. Particles further into the flow, in the rectangular box shown, performed the motion basically characteristic of the flow, namely motion towards the piston followed by an inward motion away from the piston. No rolling up ensued. The envelope of the particles at increasing times is indicated on figure 3 and particle paths are also shown. Further work showed that certain particle streaks did in fact roll up a little indicating that the observed circulating motion is partly a character of the basic flow and not entirely due to a concentrated vortex motion. The computed effect is not by any means sufficient to account for the rotation observed. At this stage of the work it appeared that repetition with smaller mesh and larger values of $h^2Re/\Delta t$ might produce greater accuracy and better agreement with experiment. It was thought that further improvement might be obtained by iterating to obtain the stream function more accurately. This was not found to be the case!

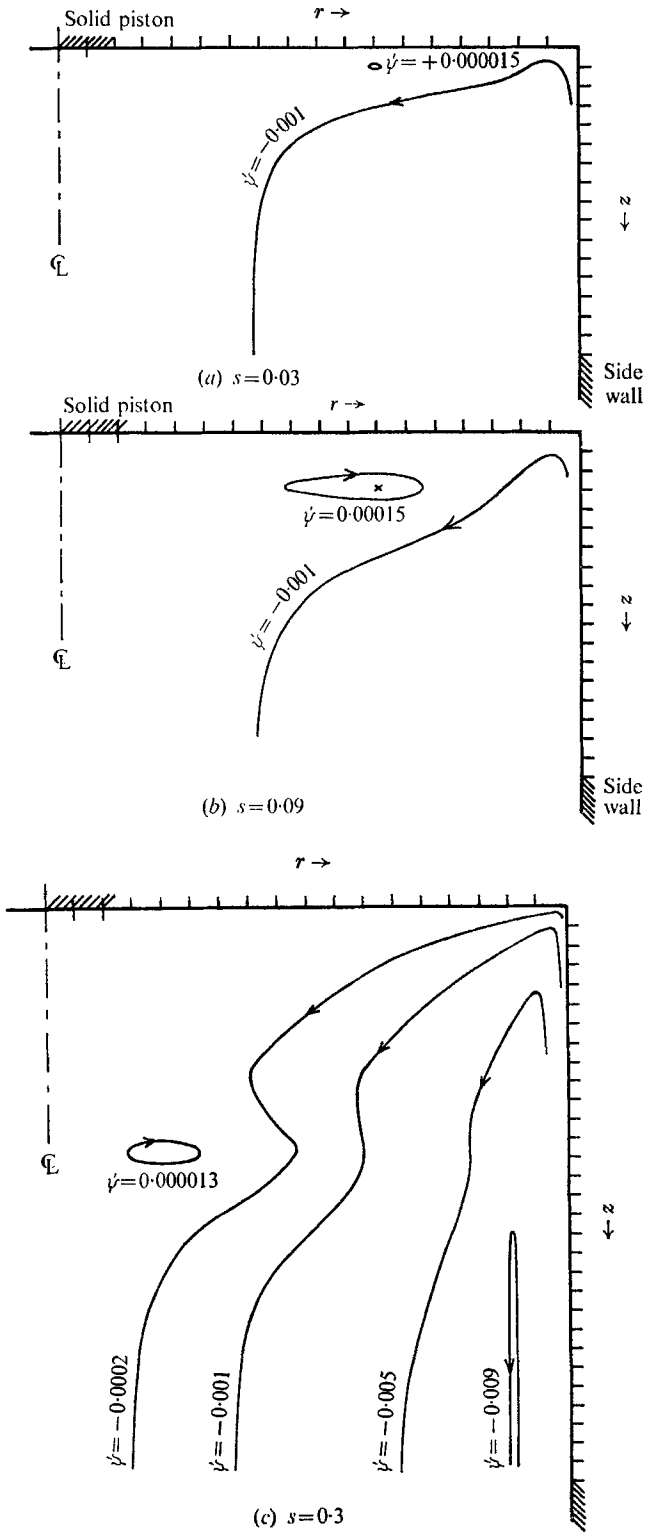

FIGURE 1(*a*) to (*c*). For legend see facing page.

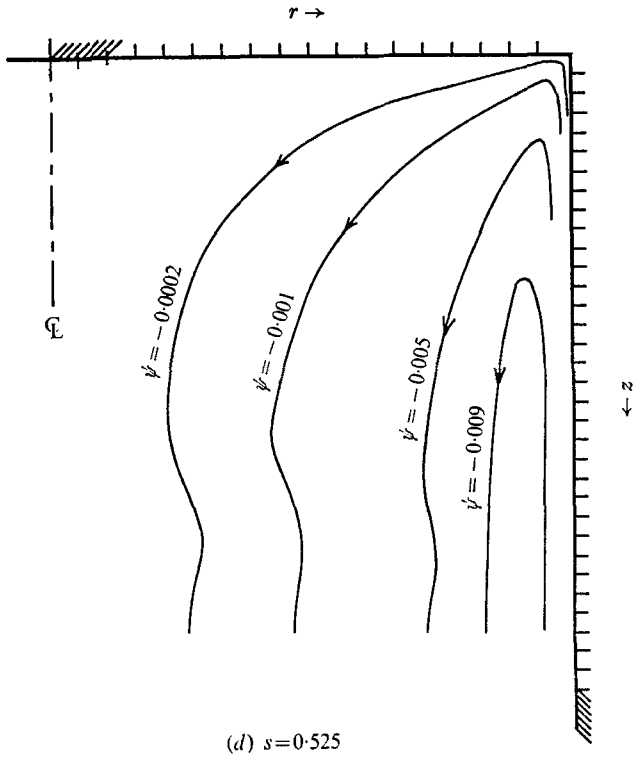

FIGURE 1. Piston started impulsively to $Re = 1000$, contours of constant stream function ψ relative to the piston or instantaneous streamlines relative to the piston. Axial mesh $g = 0{\cdot}02$, radial mesh $h = 0{\cdot}027$. s = diameters of piston travel, $\Delta t = 0{\cdot}003$, $h^2Re/\Delta t = 270$.

8. Computation with random disturbance included

Consider again the iteration to obtain the stream function. Iteration is performed if the maximum change in ψ at any mesh point is greater than a prescribed limit and iteration continues until the maximum change in any one iteration is less than this limit. Most work was done with this limit for the change in ψ equal to 0·0002. The number of iterations n was counted and could be displayed. It is found that n decreases with time and is only large for the first few time steps and that there usually is no iteration after the order of 10 time steps. Making the limit for change in stream function large is equivalent to subjecting the flow to initial disturbances. Any finite-difference scheme introduces some, if only slight, disturbance. Contrary to expectations it was found that decreasing the time step *reduced* the strength of the ring vortex. Decreasing the number of iterations increased the vortex strength very slightly. Since the vortex appears to weaken rather than grow stronger as the time step is decreased we conclude that it is the result of disturbances which must be written into the program to obtain the real flow. It was this discovery which led to the experiments which showed that there is a critical Reynolds number for the formation of the ring vortex.

It was considered that bumps on the wall were a likely source of disturbance. Models of bumps in the computations were found to produce strong ring vortices. These were large disturbances from which it was considered that a ring vortex could easily spring. This seemed to beg the question and this investigation was

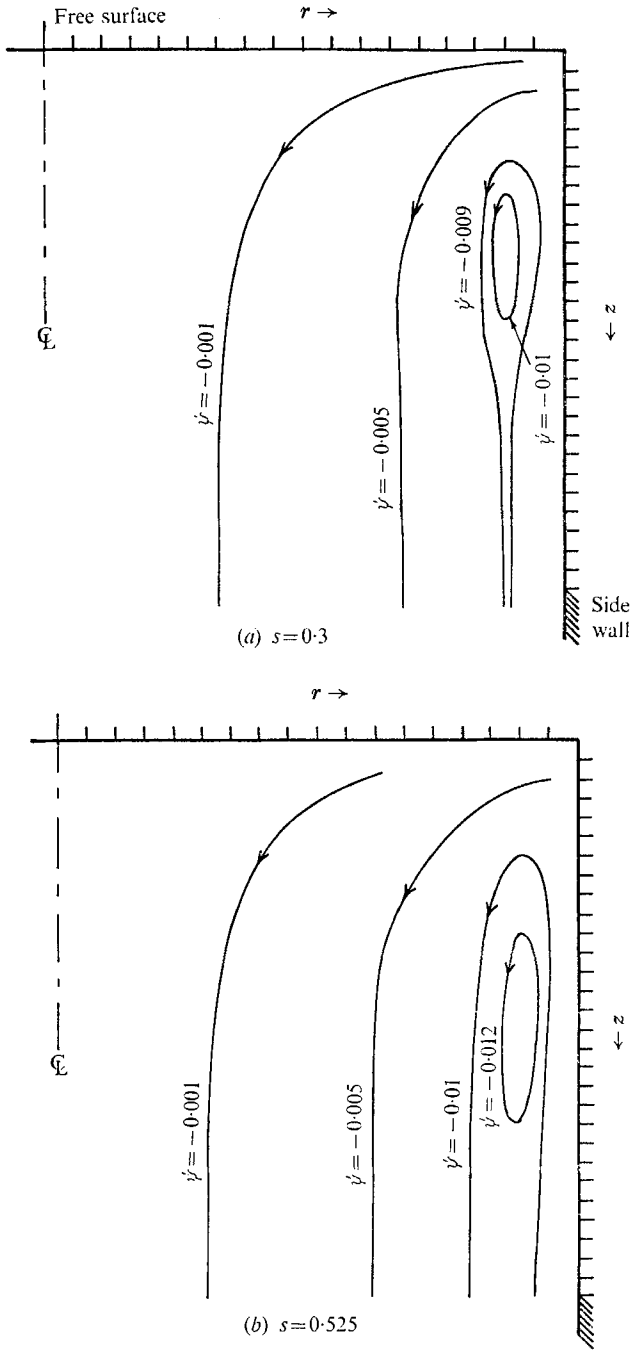

FIGURE 2. Free surface started impulsively to Re = 1000. Data as figure 1.

therefore discontinued. There was no experimental evidence that the position in the tube at which the starting flow was observed had any appreciable effect on the appearance of the flow. A random disturbance was, therefore, inserted in the computations. At each time step the stream function was randomly altered at

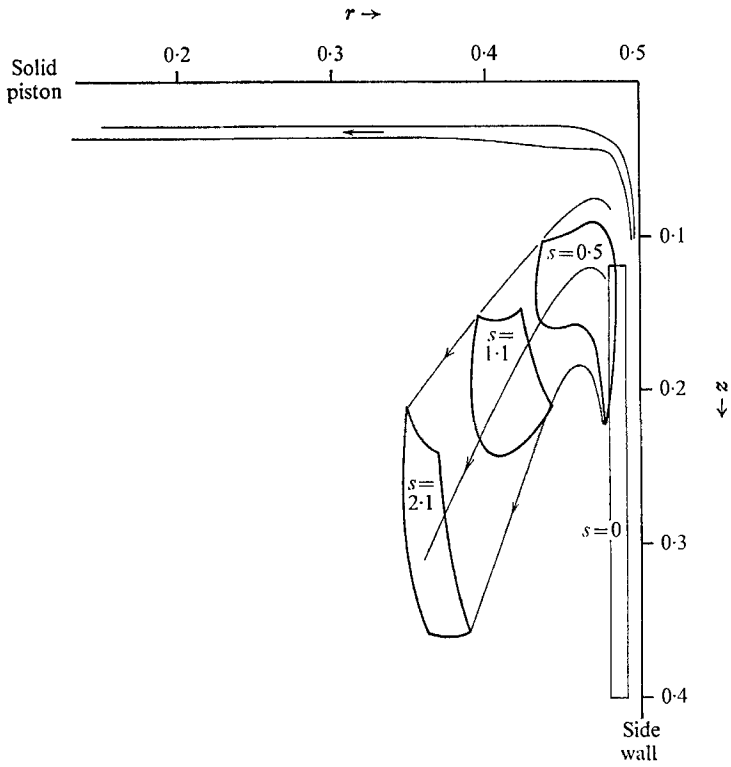

FIGURE 3. Particle tracing in front of the piston started impulsively to $Re = 1000$. Variable mesh, $\Delta t = 0{\cdot}01$, $g^2Re/\Delta t > 40$.

each interior point of the mesh. The values of the boundaries and also on the axis were not perturbed. The quantity $r\psi_0$(random) was added to the existing value of the stream function at radius r, where (random) was obtained from a repeatable random number generator with a rectangular distribution between -1 and $+1$. ψ_0 determined the level of the disturbance and was varied to produce an effect. When ψ_0 is too small it has no effect, when it is too large the resulting flow is chaotic. The value finally used was 0·02 in most cases, though this could be changed by a factor of about 4 without very significant effect.

The applied disturbance can be thought of as modelling an added turbulent fluctuation. It is considered that an unstable flow at high enough Reynolds number when perturbed in this random way will display its unstable characteristics. It was in fact found that a systematic variation appeared in the velocity field computed. The first numerical experiments were made at a Reynolds number of 1000 which was considered to be sufficiently above the experimentally determined critical Reynolds number for instability effects to become apparent. The

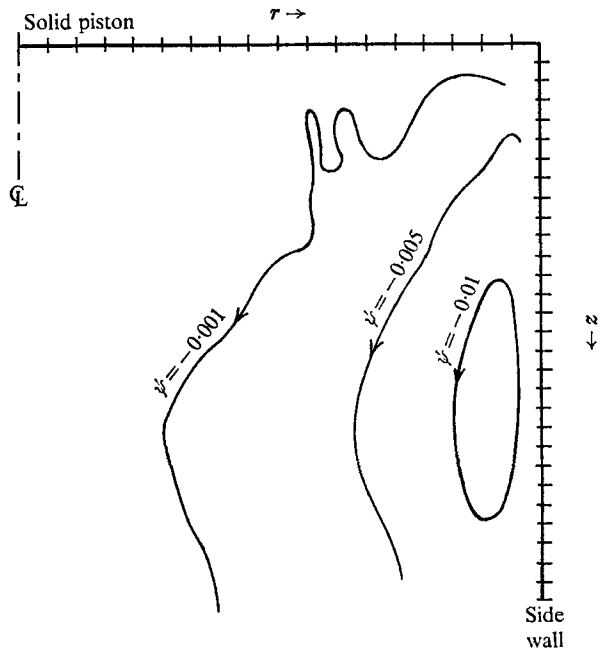

FIGURE 4. Contours of constant stream function ψ relative to the piston started impulsively to $Re = 1000$ with random disturbances added. Data as figure 1(*d*) ($s = 0{\cdot}525$). Disturbance amplitude $\psi_0 = 0{\cdot}01$.

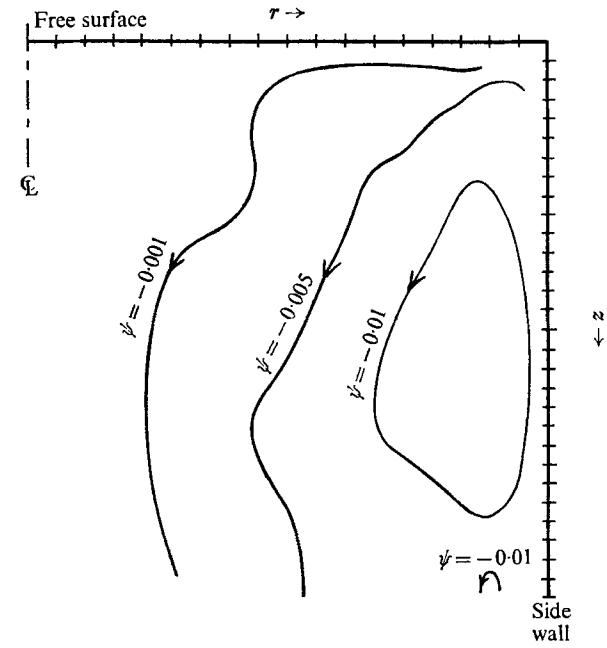

FIGURE 5. Contours of constant stream function ψ relative to the free surface started impulsively to $Re = 1000$ with random disturbances added. Data as figure 2(*b*) ($s = 0{\cdot}525$). Disturbance amplitude $\psi_0 = 0{\cdot}02$.

resulting instantaneous streamlines are shown in figures 4 and 5 which are to be compared with figures 1(*d*) and 2(*b*) respectively. In the free-surface case (figures 5 and 2(*b*)) the vortex is strengthened. When there is a solid piston a ring vortex appeared when the computation was disturbed. The detailed effect upon the velocity field is shown in figures 6 and 7. In figure 6 the change in axial

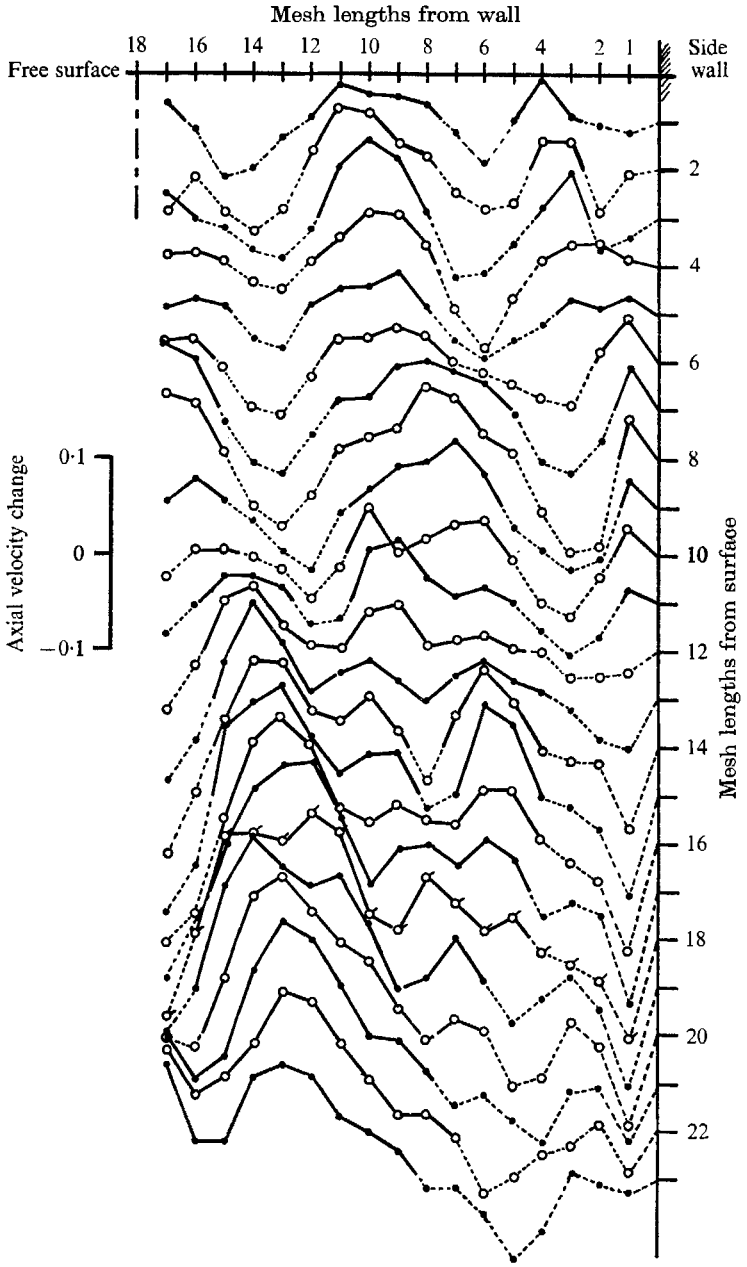

FIGURE 6. Change in the axial velocity component produced by the random disturbance, Axial velocity in figure 5 minus axial velocity in figure 2(*b*). $s = 0{\cdot}525$, $\psi_0 = 0{\cdot}02$. Intersections of the mesh with wall and surface numbered from the corner.

velocity (non-dimensionalized with the surface speed) produced by the random disturbance is plotted as a function of axial and radial position. In figure 7 the increment in radial velocity is plotted. These graphs are presented in full because there seems to be no simple way to describe the level of the random fluctuations. These may be thought of as an equivalent turbulent intensity which from observation of these figures appears to be of the order of 1 % of the piston speed. The systematic changes are an order of magnitude larger and vary smoothly with

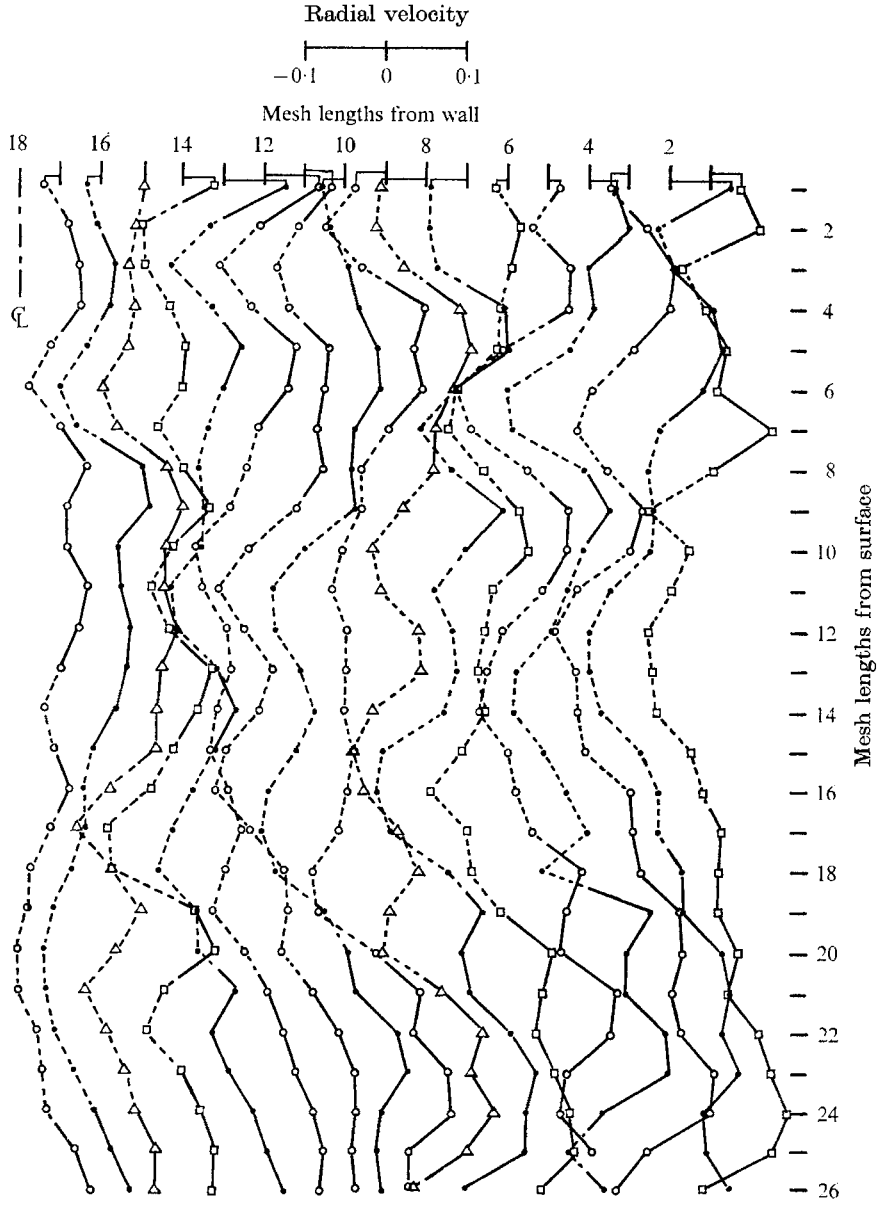

FIGURE 7. Change in radial velocity component produced by the random disturbance. As for axial component in figure 6.

position. Changing the random number generator to produce a different set of random numbers had no effect on the systematic changes observed.

It therefore appears that the ring vortex results from an instability of the flow. In the computed flow finite disturbances are necessary to trigger the instability.

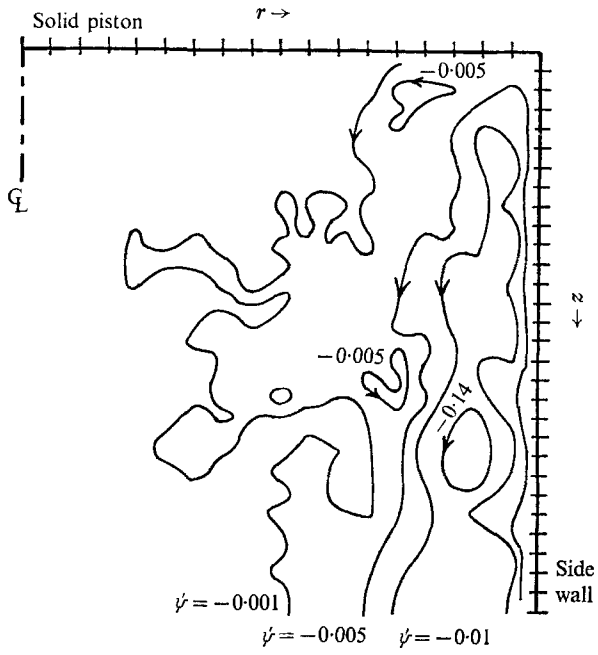

FIGURE 8. Contours of constant stream function ψ relative to the piston started impulsively to Reynolds number 525 with random disturbances added. $s = 0{\cdot}3$ diameters, disturbance amplitude $\psi_0 = 0{\cdot}02$, $\Delta t = 0{\cdot}0015$, axial mesh $g = 0{\cdot}02$, radial mesh $h = 0{\cdot}027$.

The obvious questions arise. Would the real flow show the ring vortex if disturbances were only very small and where do the disturbances come from in the real flow? The first question remains unanswered because of the experimental difficulties involved. Disturbances in the real flow can arise in at least three ways. In experiments with a solid piston its starting motion will not be smooth, some judder will be present. There are some residual motions in the fluid before the motion proper is started, but these are not expected to reach anything like 1 % of the piston speed. The walls of the cylinder will be rough. To investigate this last effect the random disturbances were injected only at those mesh points along the line one mesh interval from the wall. In the small number of cases investigated the effect was essentially the same as when the whole mesh was randomly perturbed. This is not surprising since the unstable region is close to the wall. The apparent need for the disturbances to be finite could well be due to the inability to properly model the boundary layer which for the first part of the motion is very close to the wall.

The quantitative results of Part 2 are in the form of time histories of tracer particles. Particle tracing facilities were written into the computer programs.

The comparison of computed and experimental results is made in Part 2. Some of these experiments were made at a Reynolds number of 525 which is only a little above the critical Reynolds number at which the ring vortex appears. Computation at this Reynolds number did not produce the clear indications of the vortex formation which were evident at higher Reynolds number. The turbulence level obtained for the same value of ψ_0 was considerably greater as can be seen from figure 8. Some indication of a vortex is clearly visible as well as a flow inclination towards the wall of the tube in the part of the flow remote from the piston. It is to be noted that in figure 8 the piston has only moved 0·3 diameters.

9. Determination of steady flow patterns

If the program used to determine the starting flow is continued for a very long time the steady flow in front of a piston is finally achieved. This requires a vast amount of computing time. The slow approach to the steady state is indicated by

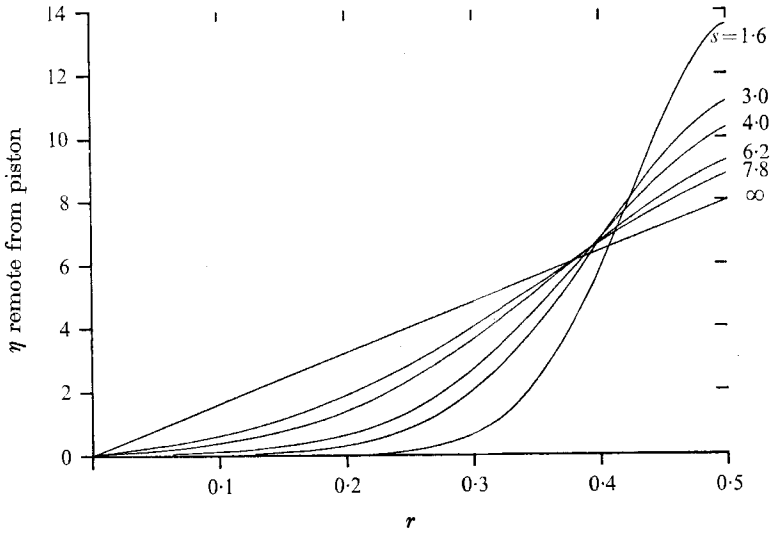

FIGURE 9. Radial distribution of vorticity as a function of time at the end of the mesh remote from the piston. Reynolds number = 525, $\Delta t = 0{\cdot}01$, $g^2Re/\Delta t > 20{\cdot}5$.

the curves in figure 9 for the one case where this was undertaken using the basic program. The purpose here was to show that the correct steady state was in fact approached. It was noticed in this long program that the closed streamlines indicated in figure 1 did reappear at later times and die away again several times. The process occurs late in the program and so could not be investigated further. To this extent a steady state seems not to be reached close to the piston. At the other end of the mesh remote from the piston it seems from figure 9 that the linear vorticity distribution is approached.

When only the steady-state value is required, considerably quicker approach to the asymptotic value is possible. If Δt is increased to the verge of computational instability the resulting flow undergoes some oscillations which die out because

of increasing computational stability with increasing time. In this way acceptable steady solutions were obtained at low Reynolds number. Increased accuracy is possible by changing to a small time step after long times when the steady state is almost achieved. Alternatively, approximation to the steady flow can be used as the starting point of the calculations.

10. Conclusions

The equations of motion for the axisymmetric flow of an incompressible fluid have been solved in finite-difference form in the manner employed previously by several other workers. The solution for flow in front of a piston started from rest in a tube exhibits the basic characteristic which is the observed flow at low Reynolds numbers. Relative to the advancing piston the flow is towards the piston at the walls and away from the piston in the centre of the tube. At higher Reynolds numbers the flow was found experimentally to possess an instability which resulted in the formation of a ring vortex.

The factors affecting the accuracy of the solution have been investigated. The major factor was found to be $h^2Re/\Delta t$, where h is the mesh length, Re the Reynolds number and Δt the time step. This factor must be high to achieve an accurate solution. It was found that the iteration strictly required to determine the new values of the stream function at each time step could be dispensed with without affecting the accuracy if $h^2Re/\Delta t$ was increased keeping $h^3Re \ll 1$. This can represent a saving in computing time. It was discovered that omitting the iteration was equivalent to a disturbance of the flow. The characteristics of the flow at high Reynolds numbers, which in practice result from instability, could be produced in the computed flow by imposing a random disturbance on the stream function at each time step. Without the random perturbation the computed and observed flows differ close to the piston. The changes affected by the perturbations are an order of magnitude larger than the perturbations and therefore real. Since artificial viscosity effects due to truncation errors are apparently absent and the Reynolds number is correctly represented one has to look for a source of these perturbations in the real flow. It is suggested that, by analogy with the transition to turbulence in boundary layers, small axisymmetric perturbations are not normally amplified to such a degree that a changed flow pattern comes into being. Amplification is a three-dimensional effect which is excluded by the present computing method and has to be introduced artificially as random disturbances. Comparison of the numerical and experimental results is made in Part 2.

REFERENCES

BATCHELOR, G. K. 1967 *An Introduction to Fluid Dynamics.* Cambridge University Press.

CHORIN, A. J. 1967 The numerical solution of the Navier–Stokes equations for an incompressible fluid. *Bull. Am. Math. Soc.* **73** (6), 928.

FROMM, J. E. & HARLOW, F. H. 1964 Dynamics and heat transfer in the Kármán wake of a rectangular cylinder. *Phys. Fluids*, **7**, 1147.

GERRARD, J. H. 1971 An experimental investigation of pulsating turbulent water flow in a tube. *J. Fluid Mech.* **46**, 43.

MACAGNO, E. O. & HUNG, T.-K. 1967 Computational and experimental study of a captive annular eddy. *J. Fluid Mech.* **28**, 43.

PEARSON, C. E. 1965 A computational method for viscous flow problems. *J. Fluid Mech.* **21**, 611.

SEXL, T. 1930 Über den von E. G. Richardson entkeckten 'Annulareffekt'. *Z. Phys.* **61**, 349.

STRAWBRIDGE, D. R. & HOOPER, G. T. J. 1968 Numerical solutions of the Navier–Stokes equations for axisymmetric flows. *J. Mech. Engng. Sci.* **10**, 389.

SYMANSKI, F. 1930 Quelques solutions exactes des équations de l'hydrodynamique de fluide visqueux dans le cas d'un tube cylindrique. *Proc. 3rd Int. Congr. Appl. Mech.* **1**, 249.

THOM, A. 1928 An investigation of fluid flow in two dimensions. *Aero. Res. Counc. Rep. & Memo.* 1194.

THOMAN, D. C. & SZEWCZYK, A. A. 1964 Time-dependent viscous flow over a circular cylinder. *Phys. Fluids*, **12**, II-76.

UCHIDA, S. 1956 The pulsating viscous flow superposed on the steady motion of incompressible fluid in a circular pipe. *Z. angew. Math. Phys.* **7**, 403.

WILLIAMS, G. P. 1969 Numerical integration of the three-dimensional Navier–Stokes equations for incompressible flow. *J. Fluid Mech.* **37**, 727.

WOMERSLEY, J. R. 1955 Oscillating motion of a viscous fluid in a thin walled elastic tube. *Phil. Mag.* **46**, 199.